Transportation Infrastructure Geotechnology (2022) 9:133–154
https://doi.org/10.1007/s40515-021-00159-6

TECHNICAL PAPER

An Extension to Barcelona Basic Model Predicting the Behavior of Unsaturated Soils

Alireza Sadeghabadi[1] · Ali Noorzad[2] · Amirali Zad[1]

Accepted: 1 March 2021/Published online: 4 April 2021

Abstract

Slope failures along highways can highly affect the stability of road structure. In this respect, the analysis of the wetting process in unsaturated media is of great importance to slopes and pavements. In this study, the Barcelona basic model (BBM) was implemented in finite difference-based program to investigate the geomechanical behavior of fine-grained unsaturated soils subjected to wetting. This numerical modeling has been verified against some data in the literature. The application of the model was investigated for the response of a compacted fill slope involving suction-induced problems. The study also considered the effect of the over-consolidation ratio (OCR) in unsaturated soils, especially stress paths, as a modification to BBM. The simulations also include using BBM and modified BBM in FLAC to evaluate the response of deep soil mixing (DSM) improvement method in subsurface areas of the pavements in unsaturated media. Finally, modified BBM codes in the finite-difference program were presented for dealing with problems associated with soil slope and the DSM method to improve the foundation of pavements. Also, over-consolidation ratio has been added to BBM to optimize its application in suction various processes. Overall, it has been found that the modified BBM leads to more occurred results.

Keywords Road construction · Barcelona basic model · Unsaturated soil · Over-consolidation ratio · Soil improvement · Finite difference analysis · Soft soil

✉ Ali Noorzad
a_noorzad@sbu.ac.ir

Alireza Sadeghabadi
ali.sadeghabadi.eng@iauctb.ac.ir

Amirali Zad
a.zad@iauctb.ac.ir

[1] Department of Civil Engineering, Central Tehran Branch, Islamic Azad University, Tehran, Iran

[2] Faculty of Civil, Water & Environmental Engineering, Shahid Beheshti University, Tehran, Iran

1 Introduction

The face for highways, roads, earth dams, stockpiles, and retaining walls are constructed in adjacent to slopes subjected to the lateral forces of the soil mass. Soil slope stabilization is the process of improving the shear strength parameters of soil and thus increasing safety against failure (Li and Aubetin 2010). In road construction, this method is used to reduce permeability and compressibility of the soil mass in earth structures and to increase its shear strength. Since the wetting-induced process takes place in the soil, the geomechanical behavior of unsaturated soils in the design of structure should be considered. Constitutive modeling of unsaturated soils has been the subject of many recent studies (Wheeler et al. 2003; Sheng et al. 2004; Nuth and Laloui 2008; Zhang and Lytton 2009a, 2009b; Zheng and Lytton 2012; Sheng and Zhou 2011; Hatami and Tourchi 2018). However, sophisticated constitutive models have been seldomly implemented in computer programs for practical applications due to the complexity of those models. Among many developed constitutive models, Barcelona basic model (BBM) has been used in the present research. It utilizes the critical state concept capable of simulating unsaturated soils behavior along with suction loading variations.

BBM is a geomechanical constitutive model for capturing the elastoplastic behavior of unsaturated soils. The model was first developed in the early 1990s as an extension of the modified Cam-Clay (MCC) model to unsaturated soil conditions (Alonso et al. 1990). BBM can describe several typical features of unsaturated-soil mechanical behavior, including wetting-induced swelling and collapse strains, depending on the magnitude of applied stresses (Fredlund et al. 2012). Moreover, it can predict the increase in shear strength and apparent pre-consolidation stress with suction (Gens et al. 2006). Several studies have been conducted to investigate the behavior of unsaturated soils utilizing laboratory tests (Hoyos et al. 2012; Mun and McCarthney 2015; Xiong et al. 2019). However, fewer studies have been focused the wetting-induced volumetric strain behavior (Cerato et al. 2009). Saffih-Hdadi et al. (2009) determined that most types of compacted soils might be subjected to failure under normal conditions (Jayanth et al. 2012).

Figure 1 represents the 3D yield surface in $\overline{p}$–q–s space, where $\overline{p}$ is the net mean stress (i.e., total stress minus air phase pressure), q is the shear stress, and s is matric suction. In this approach, both saturated and unsaturated conditions are simulated. In two fluid phase conditions, the primary variable is air pressure, which is greater than water pressure (Vanapalli and Oh 2014). Thus, for fully saturated cases versus unsaturated cases, the geomechanical behavior depends on two stress variables, namely net mean stress and matric suction defined in Eqs. (1) and (2), respectively. Moreover, in this research, an elastoplastic version of BBM is implemented in FLAC. It is of note that the soil strength in this model is a function of both suction variations and net stress. In this approach, an existing module for MCC model in FLAC^{2D} is extended, and a function as a computational solution for suction-dependent strain and net stress (i.e., total stress minus air pressure: $\sigma_t - \sigma_a$) in unsaturated medium has been presented. Fine-grained soils in earthen structures such as slopes are usually under an unsaturated condition. Therefore, a centrifuge model (Hatami and Miller 2013) was employed to simulate the suction response of a compacted model as a fill embankment slope to evaluate displacements in the model. The wetting-induced processes of these structures can occur due to rising the water table.

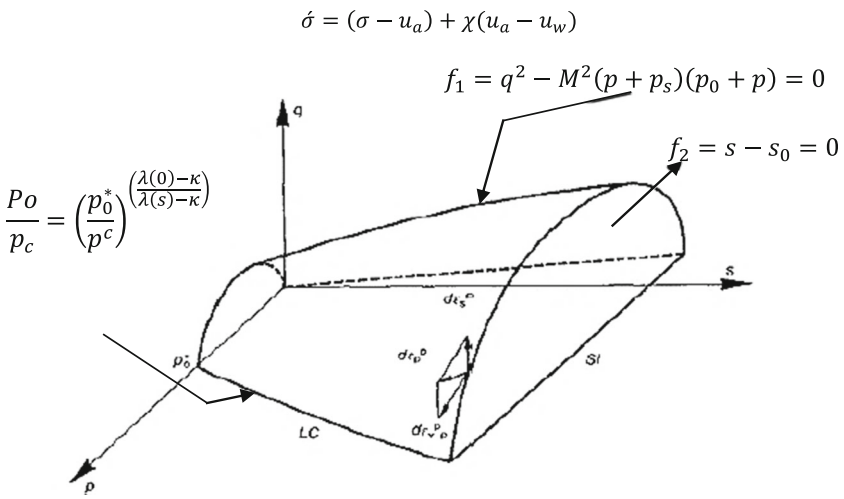

Fig. 1 The 3D illustration of the yield surface in BBM (After Alonso et al. 1990)

Lateral displacement and settlement of embankments are common problems that cause failures in slopes. In this research, volumetric strain change behavior in various confining stresses concerning loading collapse (LC) is investigated as well. In the next step, the effect of over-consolidation ratio (OCR) has been investigated, and a modification into a part of the model relations has been proposed. Stress paths are generated for two cases including BBM and modified BBM which have been implemented in FISH codes, followed by comparing them with experimental results of Alonso's research. In the final section, a deep soil mixing (DSM) system as a ground improvement that can be applied in pavements has been investigated in an unsaturated medium using the finite-difference modeling (FDM). Suitable materials for the DSM system contain compacted soils in low suction values during the wetting-induced process.

2 Formulations of BBM

A well-known sample for a single stress measured for unsaturated soils is named Bishop's stress (Bishop 1959):

$$\sigma = (\sigma - u_a) + \chi(u_a - u_w) \tag{1}$$

where u_a is the pore air pressure, u_w is the pore water pressure, and χ is a factor dependent on the degree of saturation. Its value is 1 and 0 at full saturation and dry soil, respectively. BBM is formulated in triaxial stress space using the MCCM model as the underlying model for the saturated condition. Under isotropic stress states, the relevant stress variables in the BBM are the mean net stress $\overline{p}$ and matrix suction s, defined as follows (Alonso et al. 1999):

$$\overline{p} = p - u_a \tag{2}$$

$$s = u_a - u_w \tag{3}$$

where $\overline{p}$ is the net mean stress. In contrast to the MCC, BBM has a nonassociated flow rule. Therefore, while the stress condition is on the yield surface, the plastic strains are estimated using the plastic flow rule:

$$d\varepsilon_i^{p-LC} = \Lambda_1 \cdot \frac{\partial Q_1}{\partial \sigma_i^*} \tag{4}$$

where $d\varepsilon_i^{p-LC}$ denotes a principal rate of plastic strain due to yielding on LC, Λ_1 is a plastic multiplier, and Q_1 is the plastic potential function to be applied in conjunction with f_1 (Figure 1).

Post-yield compression curves at different values of suction define a series of isotropic normal compression lines in the $v-p$ plane. In this regard, normal compression line (NCL) at any constant suction s can be mathematically expressed as the following equation:

$$v = N(s) - \lambda(s) ln \frac{\overline{p}}{p^c} \tag{5}$$

where intercept $N(s)$ and gradient $\lambda(s)$ are both functions of suction (Fig. 2a). Also, $\lambda(s)$ is a compressibility parameter in intact soil states at suction s:

$$\lambda(s) = \lambda(0)[(1-r)\exp(-\beta s) + r] \tag{6}$$

In Eq. (6), as another empirical relation, $\lambda(s)$ specifies the shape of the LC yield surface, which increases in size with matric suction. The maximum increase in soil stiffness with suction is defined as β. The intercept $N(s)$ in Eq. (5) is defined at $\overline{p} = 1$ kPa and is not the same as the intercept defined by Alonso et al. (1990) and Josa (1988) at a reference pressure p^c. By combining Eqs. (5) and (6), the shape of the LC yield curve can be obtained in the plane and the development of this shape during yield curve expansion as:

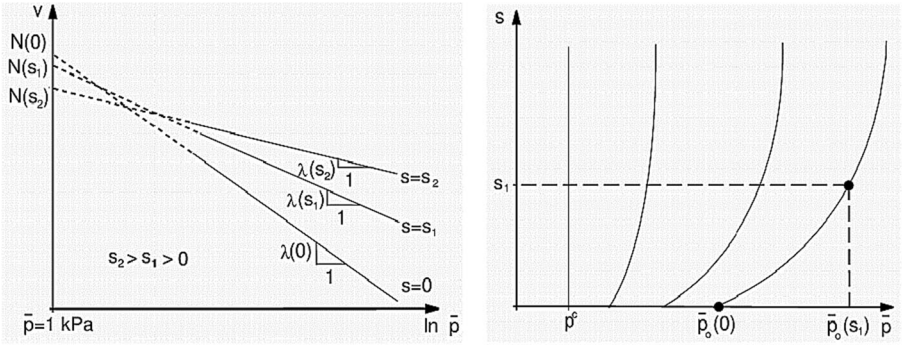

Fig. 2 **a** Post-yield compression curves at different values of suctions and **b** the shape of the LC yield curve in the $\overline{p}-s$ plane (Wheeler et al. 2003)

$$\frac{po}{p^c} = \left(\frac{p_0^*}{p^c}\right)^{\left(\frac{\lambda(0)-\kappa}{\lambda(s)-\kappa}\right)} \quad \frac{\overline{p}_0(s)}{p^c} = \left(\frac{\overline{p}_0(0)}{p^c}\right)^{\left(\frac{\lambda(0)-\kappa}{\lambda(s)-k}\right)} \tag{7}$$

where $\overline{p}_0$(s) is the isotropic yield value of $\overline{p}$ at a general suction "s" (Fig. 2b), $\overline{p}_0(0)$ is the value of $\overline{p}_0$(s) at zero suction which defines by the interception of the yield curve with the $\overline{p}$ axis, and p^c is an additional soil constant equal to $p_0(0)$. A major assumption of Alonso et al. (1990) and Gens and Josa (1988) in deriving Eq. (7) is that the developing shape of the yield curve as it expanded could be traced back to a situation where the yield curve would be a straight vertical line in the $\overline{p}$–s plane at the reference stress p^c (Figure 1b). In this equation, p_0^* is the pre-consolidation pressure at zero suction, and $\overline{p}_0(0)$ is one of the hardening parameters. As can be seen from Fig. 1b, the LC yield curve is vertical in the $\overline{p}$–s plane. When $\overline{p}_0(0) = p^c$, the yield curve becomes increasingly inclined as it expands (i.e., as $\overline{p}_0(0)$ increases). Regarding suggested unreasonable yield curve shapes for values of $\overline{p}_0(0)$ less than the reference or pre-consolidation pressure p^c, it is important to select a low value for the soil constant p^c. The locations of the normal compression lines for different values of suction (defined by Eq. 5) are linked to the developing form of the LC yield curve as it expands (defined by Eq. 7). Also, the intercept $N(s)$ of the normal compression line at a given value of suction can be expressed as:

$$N(s) = N(0) - (\lambda(0) - \lambda(s))\ln p^c - \kappa_s \ln\left(\frac{S + P_{at}}{P_{at}}\right) \tag{8}$$

where $N(0)$ is the corresponding intercept at zero suction. The seven soil constants required to model behavior under isotropic stress states with the BBM are therefore κ, κ_s, $\lambda(0)$, $N(0)$, r, β, and p^c. Three further constants are required to complete the model for triaxial stress states.

3 Verification of BBM Implementation in FLAC

Numerical simulations were conducted for self-weight, complete saturation, and suction variation condition, followed by verifying the implementation of BBM in FISH using analytical solutions in the literature. FISH is a programming language embedded within FLAC that enables the user t to define new variables and functions. These functions may be used to extend FLAC's usefulness or add user-defined features.

In FISH, new variable states and special grid generators are implemented. Also, servo control may be applied to numerical modeling (Ho and Hesieh 2018). BBM parameters for the numerical simulation were selected from Alonso's research and summarized in Table 1. It is of note that the suction-induced paths due to the wetting process are simulated by suction decrement from a determined value to the least (i.e., 200 kPa to 0). This numerical analysis can simulate the reduction changes in suction in a relatively simple way. Figure 3 demonstrates stress paths by volumetric deformation due to the wetting process from Alonso's experimental study. As can be seen, path

ABFH occurs inside the elastic region and induces a little swelling. In stress path AEFH, the sample was condensed to the specific value for net mean stress. In this path, specific volume decreases from 1.82 to 1.76. Similarly, path AEGH starts at a confining pressure of 600 kPa and leads to a specific volume reduction from 1.79 to 1.73.

In the elastic medium, the soil sample has experienced a low value of swelling for smaller stresses. On the other hand, after yielding at bigger stress planes, the curve would fall. A comparison of the results (Fig. 4) indicates a good agreement between the predicted (Alonso et al. 1990) and analytical results obtained by using FLAC for both magnitudes and trends.

In Figs. 5 and 6, stress paths ACEFH, ACEGH, and BDFH obtained from wetting-induced paths of AB, EF, and GH, respectively, are compared with those of Alonso's research in similar cases. Using this approach allows modeling the reduction in matric suction in a comparatively simple manner.

3.1 Numerical Modeling of an Unsaturated Soil Slope

To evaluate the proposed model, we considered a soil slope that is a part of highway design in different stages of construction and various suction contents. BBM parameters for the reference soil reported by Alonso et al. (1990) are summarized in Tables 1 and 2. These tables present the numerical results for a model surface and centerlines' settlements.

The stress paths discussed earlier are most commonly used to determine parameters obtained from some isotopically triaxial tests proposed by Alonso et al. (1990). In this section, a compacted kaolin (CK) from (Josa 1988; Alonso et al. 1990) with given BBM parameters was selected as the model properties. This type of soil is categorized as a symbol group of ML (silt) in ASTM D-2487. Figure 7 shows the geometry and finite-difference grid for the embankment model. The Mohr-Coulomb model (MC) was utilized to simulate the behavior of the saturated part of the structure (i.e., foundation). The height of the model was 10 m with a slope of 1:2 (Sheng et al. 2004).

The model centerline was placed at the embankment crown along the boundary lines. The embankment wings are fixed for lateral displacement. However, on the bottom side, both displacements in the x and y directions are fixed. The model was simulated using the BBM relations with an initial suction amount of 100 kPa. In the first step of the model construction, the foundation reached equilibrium under its weight because of gravitational stress. In real circumstances, the embankment was constructed

Table 1 BBM parameters as collected from Alonso et al. (1990)

Soil type	Compressibility under stress changes					Compressibility under suction changes					Reference stress parameters	
	λo	κ(κ)	β $(MPa)^{-1}$	r	P^c MPa	λs	κs	G MPa	M	k	Pp_o	S_o MPa
CK1	0.14	0.015	16.4	0.26	0.043	0.05	0.01	3.3	0.82	1.24	0.055	0.03
CK1	Compacted kaolin											

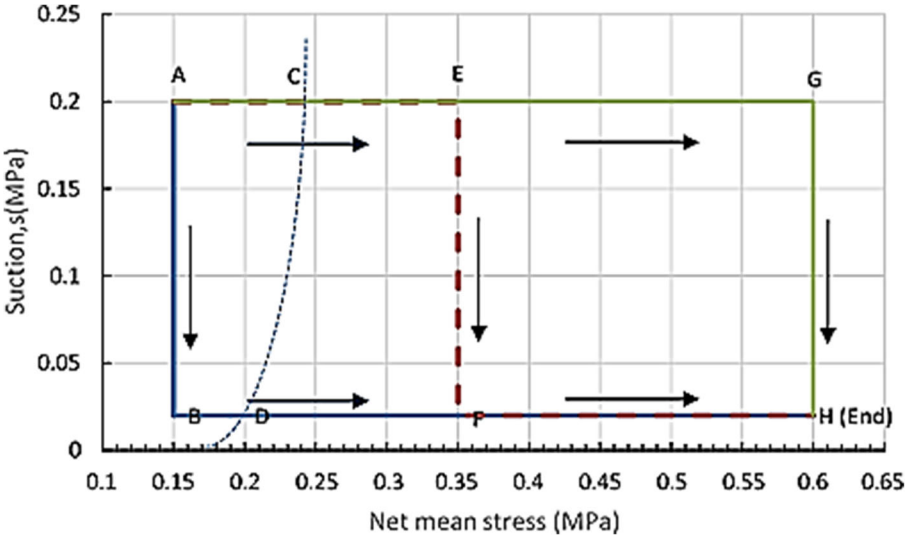

Fig. 3 Stress paths in a case study (Alonso et al. 1990)

in 10 steps, considering the initial suction of 100 kPa. While suction value alters from the amount of 100 kPa to zero, the whole embankment is subjected to impermanent equilibrium. In other words, the 10-m embankment was simulated by FLAC in 10 stages to demonstrate the common construction method.

3.2 Result and Discussions

The BBM implemented in FLAC has been verified using analytical solutions and with those in similar conditions in the literature. Figure 8 depicts displacement vectors in the embankment model at equilibrium conditions after self-

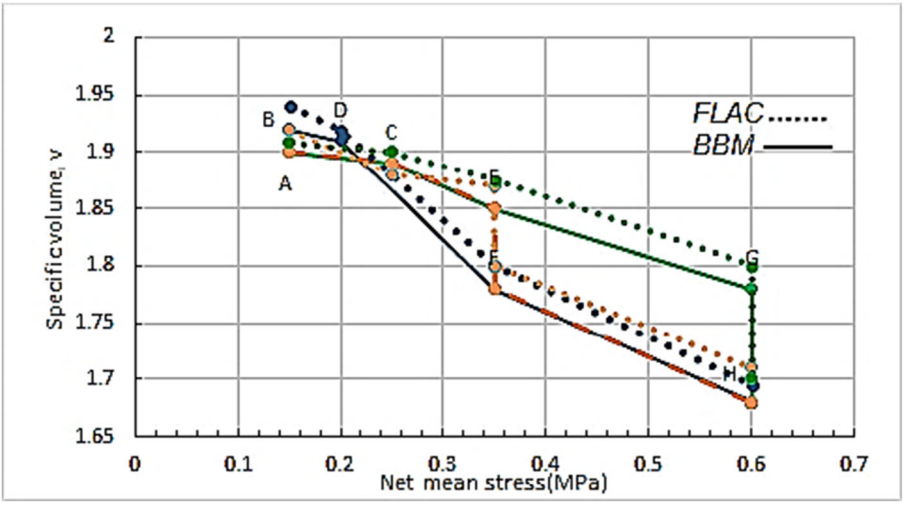

Fig. 4 Comparison of FLAC predicted and BBM analytical results in the stress paths

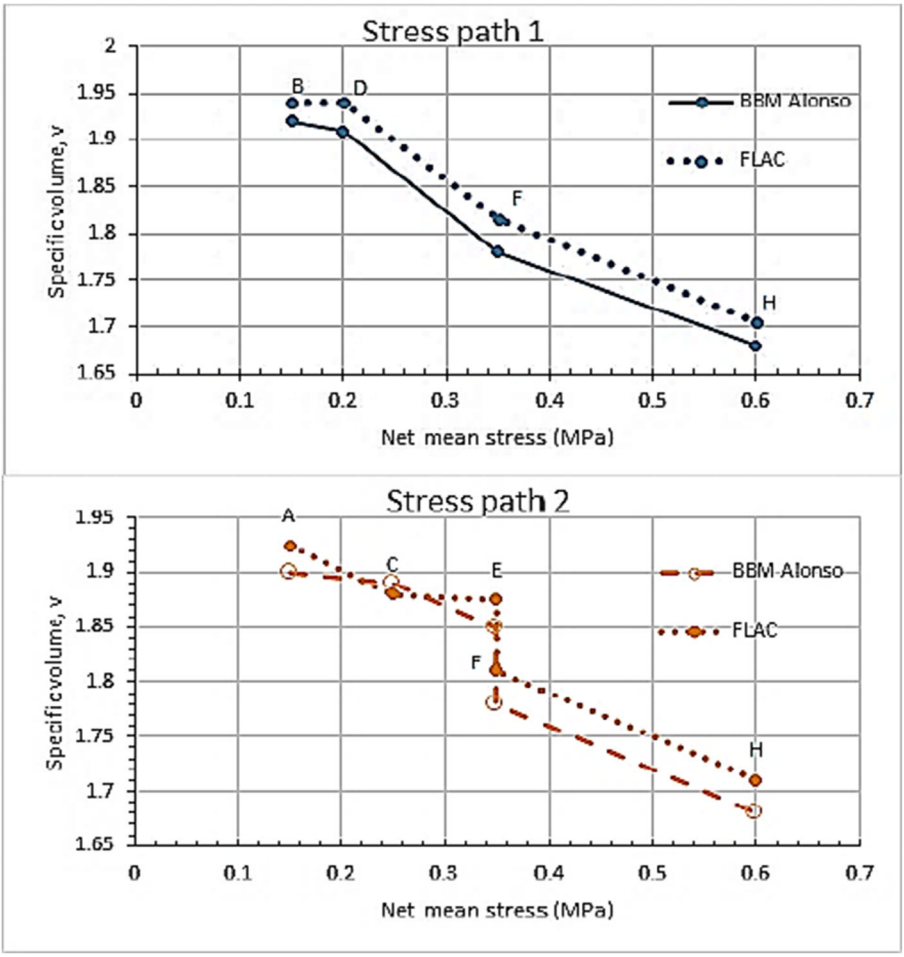

Fig. 5 Comparative scatter diagrams of FLAC results and Alonso's research cases 1 and 2

weight loading and full saturation in the literature (Gallipoli et al. 2010; Zhang and Xiao 2013). Figure 9 displays the model plots as the result of BBM codes implementation in FLAC under the same conditions.

In the present study, these y-direction displacements are 47 mm and 163 mm, respectively, which are almost similar to those reported in the literature. Also, the total amounts of maximum displacement vector in previous studies (Zhang and Xiao 2013) and the present research are 209 and 191 mm, respectively, indicating their good agreement. The parameters were used in the modeling approach are represented in Table 2.

To better study the BBM implementation in FISH codes, settlements and lateral displacements in different cases have been evaluated to verify the results of this study compared to those of published literature. Figure 10 depicts a comparative scatter diagram for settlements of embankment surfaces at different distances from the centerline. As can be seen, following the complete

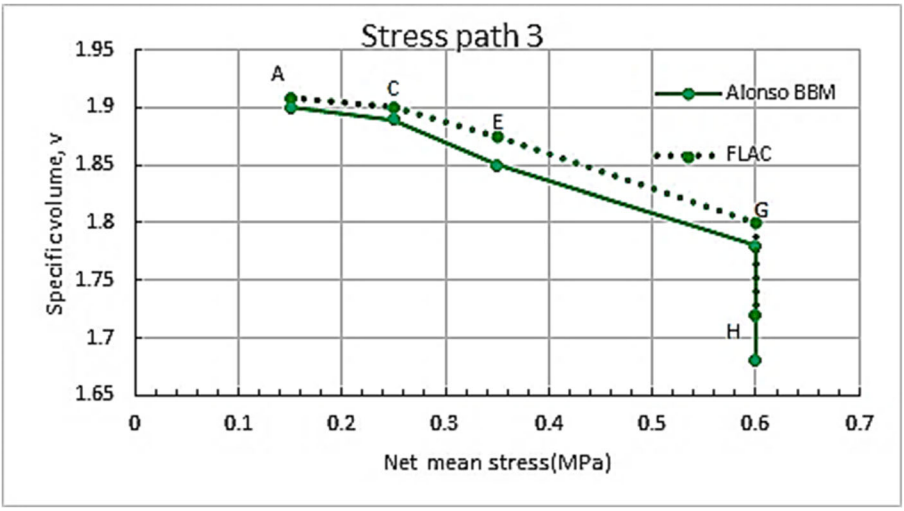

Fig. 6 Comparative scatters of FLAC results and Alonso's research case 3

saturation, the settlement of the embankment surface is approximately two or three times larger than that at the last situation. This settlement has reached 250 mm and 239 mm in this study and the literature, respectively. Hence, the value of the suction-induced settlement is almost 190 mm. Figure 9 represents the settlement along the longitudinal stages of the embankment in three conditions, self-weight loading, full saturation, and wetting process. As can be inferred from Fig. 10, the results for y-displacements of the embankment in different cases of the present study are in close agreement with those of the selected published papers (Hatami and Miller 2013).

In Fig. 11 settlement levels of the embankment at a different elevation have been plotted. In both the literature (Zhang and Xiao 2013) and BBM implementation into FLAC in this research, the maximum settlement regarding self-weight occurred at mid-height of the embankment. The reason is that the model was constructed gradually, and the accumulative displacement was reported since the placement of each level. The results in both studies match very well and specifically show the acceptable performance of FISH programming in this study.

Table 2 BB-model parameters for unsaturated parts of the model (Alonso et al. 1990)

Soil type	Compressibility under stress changes					Compressibility under suction changes					Reference stress parameters	
	λo	κ(κ)	β (MPa)$^{-1}$	r	P^c M.Pa	λs	κs	G M.Pa	M	k	Pp_o	S_o (MPa)
LCT	0.066	0.008	20	0.25	0.012	0.025	0.001	7	1.2	0.8	0.02	0.3
LCT	Lower Cromer Till											

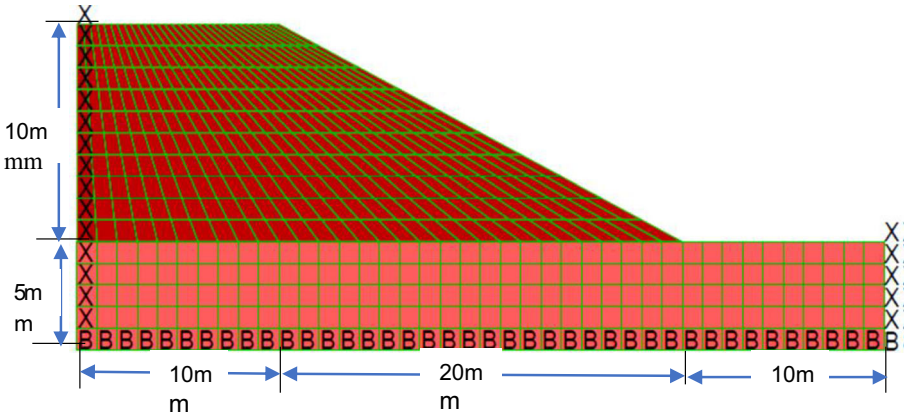

Fig. 7 Geometry and finite difference grid for the embankment model (Sheng et al. 2004)

4 Evaluation of Matric Suction and OCR in Unsaturated Earth Fill Slopes

According to the previous studies on unsaturated soils (Alonso et al. 1987, 1990), Gens et al. (2006) extended the MCC model (Roscoe and Burland 1968) to depict the stress-strain behavior and swelling of unsaturated soils. The model developed by these researchers is an improvement over BBM. Since this pioneering study, many

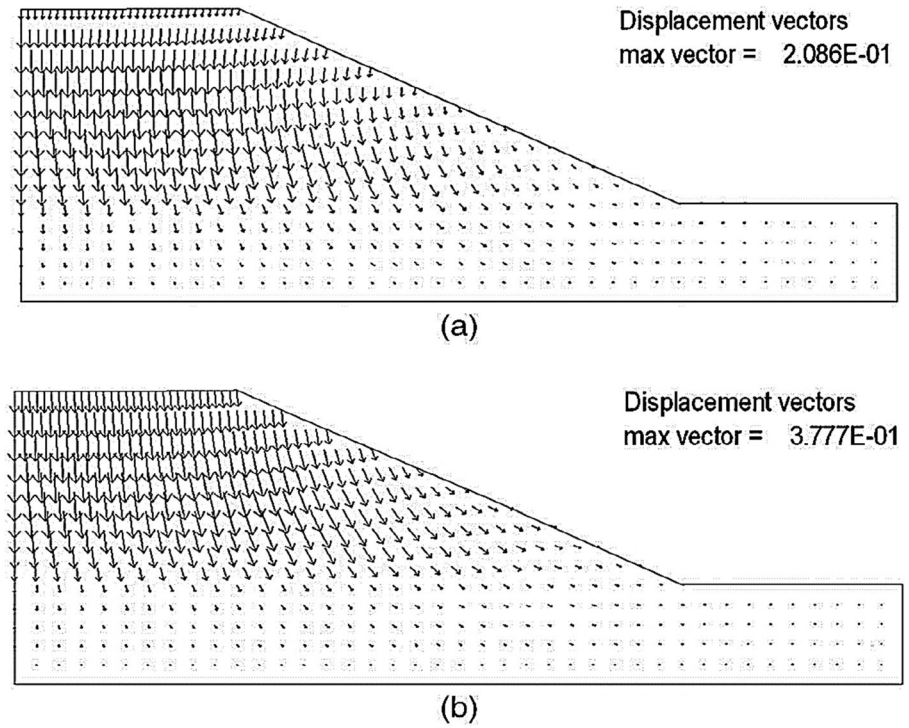

Fig. 8 Displacement vectors in two conditions (Zhang and Xiao 2013): **a** self-weight loading and **b** full saturation

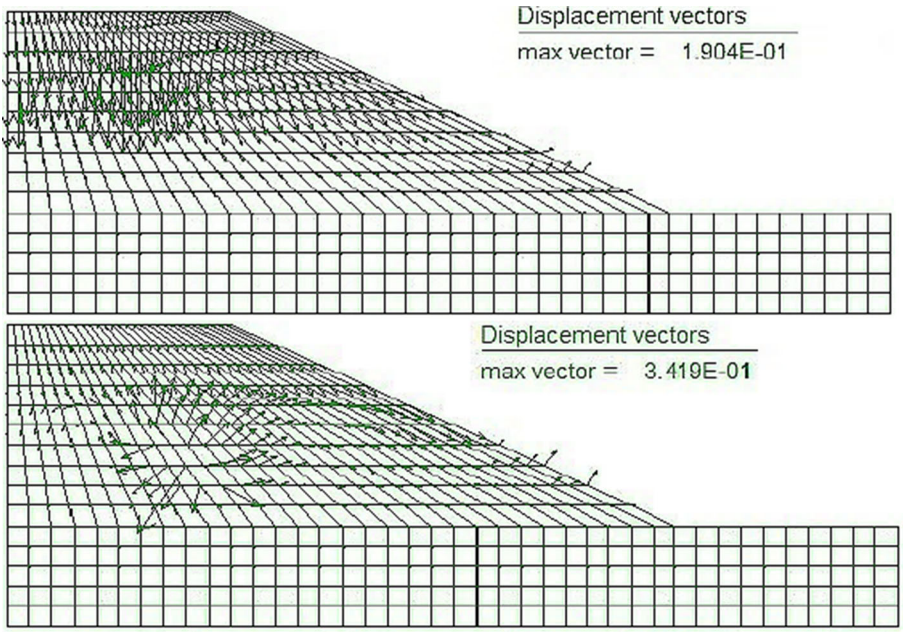

Fig. 9 Displacement vectors in two conditions (present study): **a** self-weight and **b** full saturation

researchers have concentrated on modeling the mechanical behavior of unsaturated soil. Many of these constitutive models have been developed to anticipate the stress-strain curves of normally consolidated or lightly over-consolidated unsaturated soils (Mojezi et al. 2018). However, when modeling the behavior of heavily over-consolidated unsaturated soils, the influence of the OCR on deformation in the wetting process is

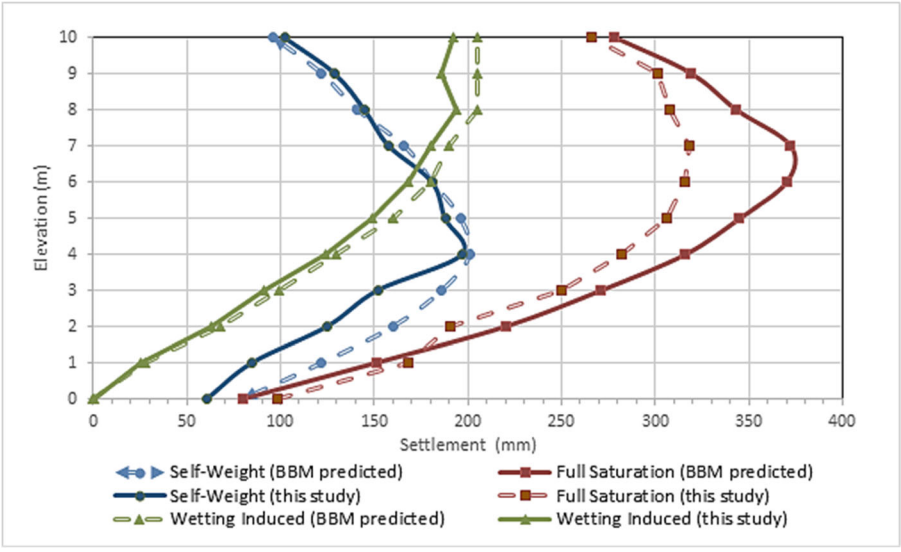

Fig. 10 Comparison of settlements in different distances from centerline in three cases including self-weight, full saturation, and wetting-induced

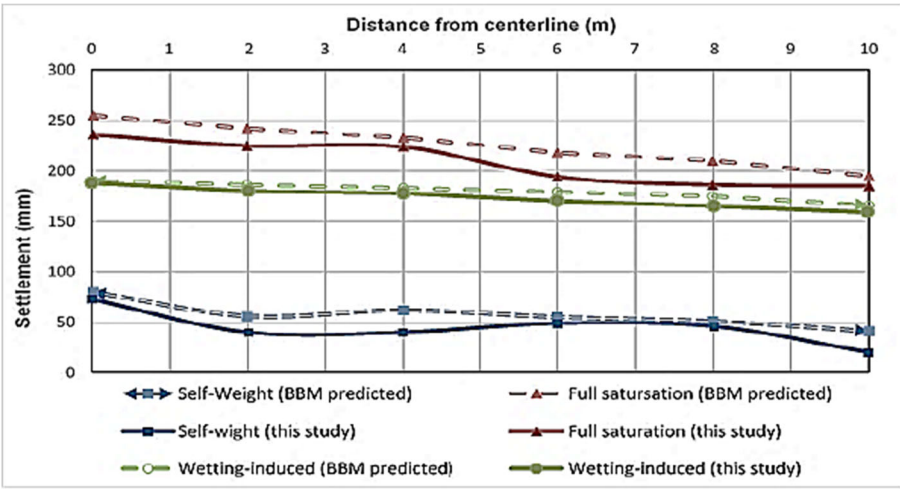

Fig. 11 Comparison of settlements in different stages in three cases of self-weight loading, full saturation, and wetting-induced

mostly overlooked. The relationship between over-consolidation stress and suction can be expressed based on the concept of stiffness parameters on normal line (NCL) in saturated state and matric suction "*s*."

Unsaturated and partially saturated soils are generally near the ground surface and are commonly over-consolidated because of environmental factors (Nishimura et al. 1999). Moreover, the climatic environment oscillation (Power and Delage 2017; Lyu et al. 2018) and human activities like excavation, tunneling, and dewatering of dams (Sheng and Xu 2011; Shen et al. 2014; Wu et al. 2015, 2017; Xu et al. 2018) alter the matric suction and stress condition in the surface soil on the ground.

As shown in Fig. 12, the compression curve inclination decreases when suction is increased in unsaturated silty clays, but the slope of the unloading curve does not change (Alonso et al. 1990). Based on the presumption that the values of plastic volume strain at points A and C are equal, the function of the loading-collapse (LC) yield curve can be derived as follows:

$$\frac{Po}{p^{c}} = \left(\frac{p_0^{*}}{p^{c}}\right)^{\left(\frac{\lambda(0)-\kappa}{\lambda(s)-\kappa}\right)} \tag{9}$$

$\frac{Po}{p_c} = \left(\frac{p_0^*}{p_c}\right)^{\left(\frac{\lambda(0)-\kappa}{\lambda(s)-\kappa}\right)}$ where p_0^* and p_0 are pre-consolidation pressures for saturated and unsaturated silty clays, respectively;κ is the slope of unloading line for unsaturated clays; $\lambda(0)$ and $\lambda(s)$ are the slopes of the compression curves for saturated clays; and p^c is the pre-consolidation stress under saturated conditions ($s = 0$). Therefore, a proposition for optimizing this equation is using the OCR as a coefficient in the LC yield function in BBM. Multiplying OCR on the right side of the equation gives:

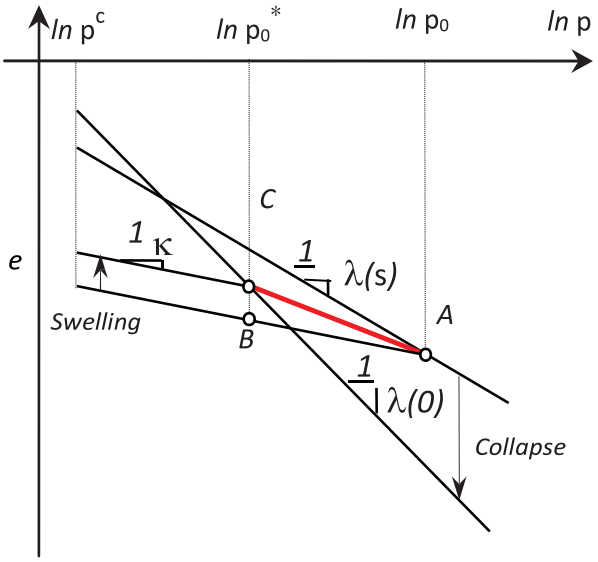

Fig. 12 The relationship between p_0^* and p_0 (Alonso et al. 1990)

$$\frac{Po}{p^c} = \left(\text{ocr}.\frac{p_0^*}{p^c}\right)^{\left(\frac{\lambda(0)-\kappa}{\lambda(s)-\kappa}\right)} \tag{10}$$

According to the experimental results in Alonso's studies, three stress paths BDFH, ACEGH, and ACEFH are investigated using a new modified form of BBM. Figure 13 compares the results of Alonso's experimental research (BBM), FLAC prediction, and modified BBM (BBM added with the OCR ratio) implemented in FLAC in the present study. Considering OCR, as a coefficient to modify loading collapse (LC) yield equation, has provided better results that match the reality compared with unmodified BBM.

A new simulation analysis of the BBM model (Hatami and Miller 2013) has been performed to verify the implementation of the modified BBM with the OCR factor. Figure 14 shows the settlement along the longitudinal stages of the embankment in three cases of analytical results (Zheng et al. 2013), BBM with normally LC equation, and modified curve with OCR factor. As presented in this figure, the curves based on the modified relation are more optimized and have a better tendency to the real situation.

Figure 15 indicates the results of a recent parametric study performed by Zhang and Xiao (2013) to investigate the influences of suction in settlement control of soil slope structures. Matric suction generally declines as approaching the groundwater. The initial matric suctions are 100 and 200 kPa. Figure 15a presents settlements of the embankment surface at different stages. The results depict that a greater level of the settlement would be anticipated for compacted kaolin placed under wetter conditions (i.e., lower initial suction) and under self-weight loading. Comparing the results of

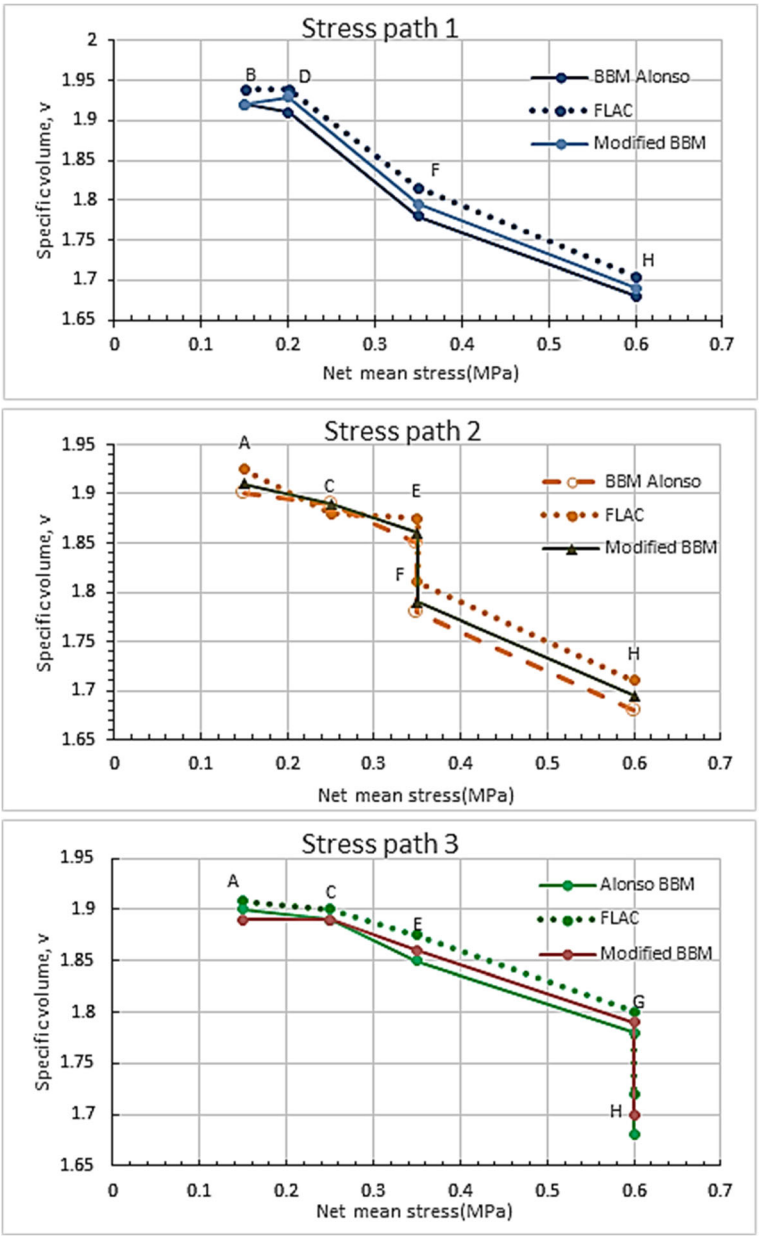

Fig. 13 Comparison of FLAC predicted, Alonso's BBM results, and modified BBM in FLAC for three stress paths

BBM and MBBM (modified BBM) implemented in FLAC with those of the previous studies has revealed that the embankment with lower initial suction is expected to undergo a greater value of the self-weight settlement. However, this amount was not as greater as these two cases, suggesting that it has not been optimized. For $S_i = 200$ kPa, the surface settlement after full saturation was approximately 80 mm larger than that for

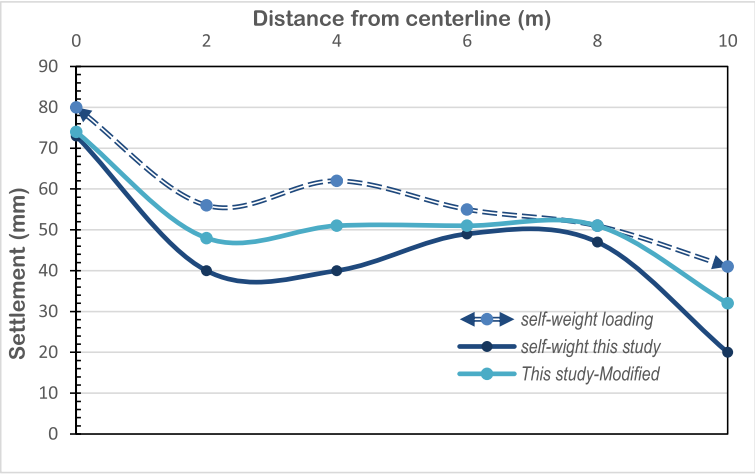

Fig. 14 Settlements of embankment surface at different distances from the centerline in three cases of model

$S_i = 100$ kPa. Meanwhile, this difference in settlements for MBBM is less than 60 mm. A lower value of settlements is another conclusion from MBBM and considering OCR in BBM formulation. As can be inferred from Fig. 15b, with increasing the initial soil suction, wetting-induced settlement of the model surface increases slightly. Using the MBBM as the constitutive model causes the soil slope surface experience less settlement. According to Fig. 15, for the BBM implementation case, the wettest unsaturated earthen slope as the main part of the road with $S_i = 100$ kPa exhibited the largest amount of settlement. Meanwhile, the model depicts the smallest amount of settlement when MBBM is considered as the constitutive model. Therefore, OCR is an effective factor for BBM modification in the wetting process of unsaturated clays in settlement control topics.

5 Evaluating DSM Column Improvement Technique in Road Construction with Unsaturated Locus

Among the soil improvement techniques, deep soil mixing (DSM) columns have been applied widely and successfully to enhance the bearing capacity and reduce the consolidation settlements of foundations in various types of road pavements. According to Rao et al. (1988), in unsaturated expansive soil, the initial stress state is measured as the corrected swell pressure from a constant volume–type odometer test. It is assumed that the ultimate water content profile of the soil stratum is near saturation at the time of full scrambling. Therefore, numerical simulations of the DSM treated sections can be carried out to find out the unsaturated DSM treated expansive soil column and surrounding untreated soil interaction. The presence of air in the pores can also increase shear strength by generating capillary suction forces (Fredlund and Rahardjo 1993) and increase the resistance of the soil to cyclic loading (Yegian et al. 2007).

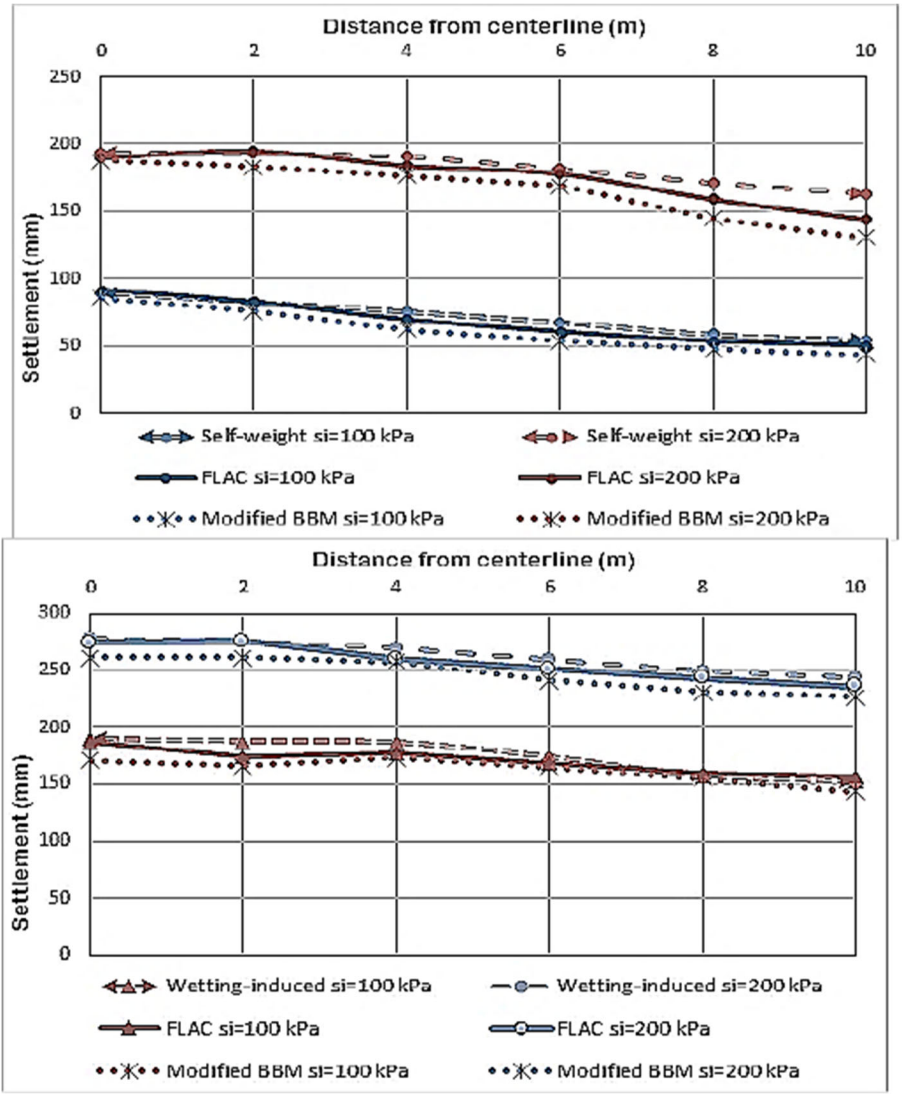

Fig. 15 Comparison of initial suction influence on settlements of model surface in three cases for **a** self-weight settlements and **b** wetting-induced settlements

5.1 Simulation of Improved Foundation with DSM in Unsaturated Media

Numerical simulations have been performed for a real model for soil in a three-phase media with different arrangements of DSM columns and full saturation condition with no ground improvement properties as the worst scenario for the foundation of road complex design (Hatami et al. 2013; Sexton and McCabe 2015). Moreover, the implemented BBM in FLAC was verified using analytical solutions in the literature. Simulation results—including model surface and centerline settlements and improved and non-improved soil complex displacements in several cases—are presented and discussed in the following. The design of foundations requires two important verifications, namely checking the

adequate bearing capacity and ensuring acceptable settlement performance. The cost-effectiveness of plans involving column-reinforced foundations constructed using various pile-like elements such as DSM is typically checked by the volumetric fraction of the material introduced into the host soil (Hosseinpour et al. 2017; Garcia 2010).

The model consists of an 80 m × 45 m and two-layer soil complex from a site investigation in southwest Iran (Alipour et al. 2016: Pakbaz and Alipour 2012). The foundation soil was simulated using the Mohr-Coulomb model, and it was assumed to be in a saturated condition. The superstructure load is equal to 120 kPa, and the width and thickness of the concrete foundation placed on this soil complex are 150 cm and 70 cm, respectively. Calibrated BBM parameters for a compacted soft clay (CK2) summarized in Table 3 were considered for unsaturated zone modeling. The compacted soil was moderately plastic and classified as ML according to the unified soil classification system (USCS). DSM columns are surrounded by a 20-m-thick layer of unsaturated soil embedded on a 25-m layer of bedrock. Three main two-dimensional plain-strain FED were modeled with three different column lengths (Table 3) using the FLAC^{2D}. Figure 16 shows these modes along with the DSM columns with 12-m length.

The unsaturated system is embedded on rocky sand which is modeled as Mohr-Coulomb (MC) in FLAC. The groundwater level is 12 m below the surface which divided the model into two fully saturated and unsaturated mediums. To comprehensively investigate the performance of columns employed in the unsaturated soil, each main model is divided into three models in which the distance between the columns varies from half a meter to 1 1/2 m. DSM columns simulated by BBM equations, implemented into finite difference codes, have been investigated in different lengths and different spacing for evaluating their capability in settlements control.

Five parameters are needed to define the MCC model, and seven additional parameters are necessary for the BBM model. In this FLAC implementation of the BBM, also, a few FISH routines, such as the one for calculating suction strain, have been developed. A function for suction alternations has been programmed with FISH codes to simulate the capability of yield functions in three-phase unsaturated zones:

$$\lambda(s) = \lambda(0)[(1-r)\exp(-\beta.s) + r] \tag{11}$$

Equation (11) explains the suction increase in the yield function. Here, $\lambda(0)$, r, and β are soil constants and key parameters controlling virgin loading under isotropic stress state.

Table 3 BBM parameters for unsaturated parts of the model as collected from Alonso et al. (1990)

Soil type	Compressibility under stress changes					Compressibility under suction changes					Reference stress parameters	
	λo	κ(κ)	β (MPa)$^{-1}$	r	P^c M.Pa	λs	κs	G M.Pa	M	k	Pp_o	S_o (MPa)
CK2	0.065	0.011	20	0.75	0.01	0.025	0.005	5.5*	1.1*	0.75*	0.04	0.07
CK1	Compacted kaolin CK2					Compacted kaolin (Barcelona clayey sand)						

*This value was not provided in the reference, and reasonable values were used in this research

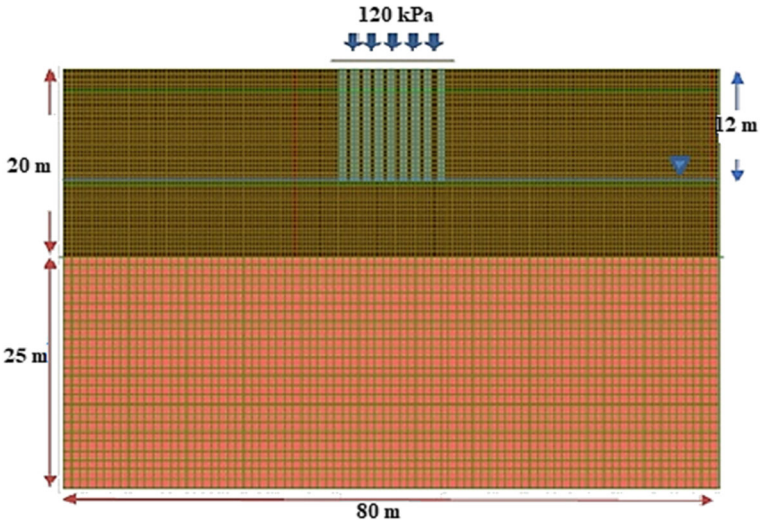

Fig. 16 Numerical model of DSM columns with a length of 12 m (case 1)

Fig. 17 depicts settlements of embankment surfaces in different column lengths and spacing summarized in Table 4 Under a uniform 120-kPa loading, the superstructure model surface settled approximately 42 mm, 50 mm, and 69 mm depending on spacings and DSM element lengths. Differences between settlement values due to the maximum and minimum of each column length are between 10 mm to 20 mm, depending on column spacing.

Furthermore, in the basic model with non-improvement properties, the maximum settlement amount reaches 120 mm. Comparison of results in Fig. 17, which has been plotted based on the data of Table 3, indicates that the longer the stabilizer length is, the less displacement in y-direction will be imposed on the structure. The results show an

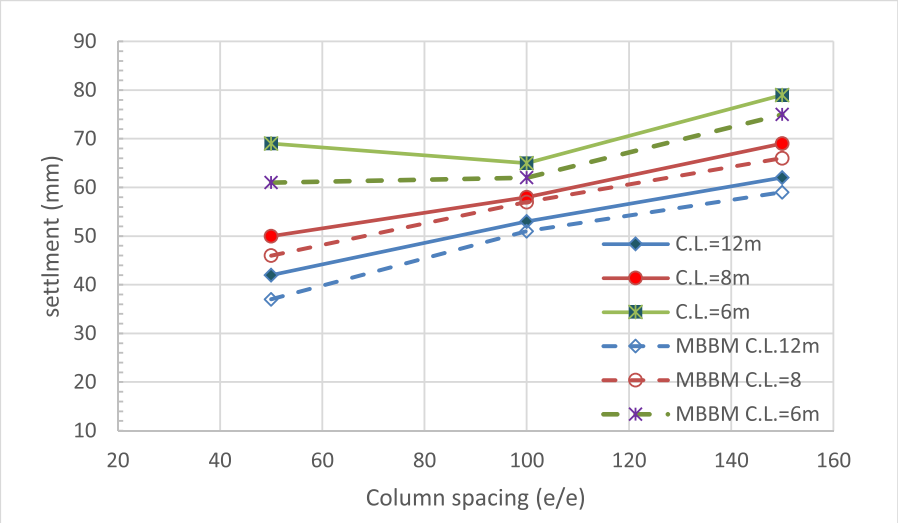

Fig. 17 Settlement of improved structure in different DSM lengths and spacings

Table 4 Different cases of DSM columns arrangements and length implemented in BBM-FLAC^{2D}

Model no.	Description	Water table from above (m)	Y-displacement (mm)	Diameter (α) (m)	Distance (cm) (edge to edge)	Column length (B)
1	Base model	12	121	1		
2	Case 1	12	42	1	50	12
3		12	53	1	100	12
4		12	62	1	150	12
5	Case 2	12	50	1	50	8
6		12	58	1	100	8
7		12	69	1	150	8
8	Case 3	12	69	1	50	6
9		12	65	1	100	6
10		12	79	1	150	6

acceptable trend in settlements from the greatest DSM column spacing (1.5 m) to the least one (0.5 m). The irrational change in the scatter diagram for the length of 6 m is likely due to a decrease in the impact of length on structural improvement. Integrating the BBM parameters into the soil improving columns gives relatively acceptable results in unsaturated soil settlement control. This is also true in other plans developed on column-reinforced foundations constructed using various pile-like elements such as an ordinary DSM system. As indicated in Fig. 17, the entire improved soil structure settles approximately 37, 46, and 61 mm. This issue represents a better response of the structure in settlement control considering BBM modified with OCR compared with other cases.

6 Conclusions

This study has aimed to investigate slope and foundation in road construction design subjected to wetting. For this purpose, an elastoplastic constitutive model based on the BBM for the mechanical behavior of unsaturated soils has been implemented into FLAC. The model was tested using several case studies. Also, analytical solutions were carried out to calibrate the finite difference model (FDM) program. Simulations of stress paths in BBM with the described algorithm in FISH indicate good agreement with Alonso's research.

Furthermore, during the wetting process, considering OCR as a modification in BBM matches better with stress paths in the original model. Hence, stress paths in yield functions of BBM (i.e., LC and SI) are among the most effective items to simulate geomechanical behavior of unsaturated soils, wetting process, and volumetric strain changes. The verified model shows a promising capability to study practical engineering programs such as the response of a slope structure subjected to suction variations. The results of this study indicated that the structure has a remarkable effect on suction-induced settlements. In the wetting process, a soil slope with higher values of initial

suction is more likely to fail due to the negative effect of matric suction. Total and differential settlements can decline meaningfully at higher suction when incorporating OCR in LC yield relation of BBM, suggesting the effective role of this factor in the mechanical and hydromechanical behavior of unsaturated soils in road construction. Settlement control and lateral displacement analysis of the model with this modified BBM make the results more adaptive to real conditions.

For example, in suction $s = 200$ kPa, surface settlement after full saturation is 80 mm more than that of 100 kPa under similar conditions. Thus, incorporating OCR in BBM leads to a 60-mm reduction in the difference between these two cases, suggesting a 20% reduction. Next, the effect of suction variations due to the degree of saturation was investigated. Moreover, the numerical modeling was utilized to study a real model covering the interaction of multiple components, compacted soils, DSM columns group, and bedrock in unsaturated media. Overall, accurate results were achieved in settlement control of this soil improvement system type for various column lengths and configurations. Besides, by applying the modified BBM model, better performance in settlement estimation was obtained with the amount of 12%, 8%, and 11.8%, respectively, for particular case with defined spacing for the columns. Therefore, BBM and MBBM implemented into FLAC^{2D} and other numerical modeling software can be used and applied to earthen slopes at any other situation related to unsaturated soil media. In this study BBM and modified BBM models have utilized for DSM columns, and the results shows better estimation of displacements using modified BBM in comparison to BBM. Future work will include an extension in FLAC to more completely model expansive clays in road construction. In unsaturated soil, suction variations are in such a close relationship with over-consolidation ratio that implementing this parameter into unsaturated models has a significant effect on both stress paths and consolidation's settlement. The results of this study can be applied to more accurate design of excavations, slopes, and pavements related to unloading/reloading cases on unsaturated over-consolidated soils.

References

Alipour R., Khazaei J.S., Pakbaz M., and Ghalandarzadeh A.: "Settlement control by deep and mass soil mixing in clayey soil." Intl Civil Engineering Institution, Paper 160008, (2016)

Alonso, E.E., Gens, A., Hight, D.W.: Special Problem Soils, General Report. Proc., 9th Eur. Conf. on Soil Mech. and Found. Engrg., Dublin. **3**, 1087–1146 (1987)

Alonso, E.E., Gens, A., Josa, A.: A constitutive model for partially saturated soil. Geotechnique. **40**(3), 405–430 (1990)

Alonso, E.E., Vaunat, J., Gens, A.: Modeling the mechanical behavior of expansive clays. Eng. Geol. **54**, 143–183 (1999)

Bishop, A.W.: The Principle of Effective Stress. Lecture delivered in Oslo, Norway, in 1955, published in: Teknish Ukeblad. **106**(39), 859–863 (1959)

Cerato, A.B., Miller, G.A., Hojjat, J.: The influence of cold size and structure on wetting-induced volume change of compacted. J. Geotech. Geoenviron. Eng. 1620–1628 (2009). https://doi.org/10.1061/(ASCE)GT.1943-5606.0000146

Fredlund D.G., Rahardjo H.:" Soil mechanics for unsaturated soils." Wiley, New York, (1993)

Fredlund, D.G., Rahardjo, H., Fredlund, M.D.: Unsaturated soil mechanics in engineering practice. John Wiley & Sons Inc. (2012)

Gallipoli, D., D'Onza, F., Wheeler, S.J.: A sequential method for selecting parameter values in the Barcelona basic model. Can. Geotech. J. **47**(11), 1175–1186 (2010)
Garcia L.M., "Influence of moisture content on pullout resistance of geotextiles in marginal quality soils." Master's thesis, Univ. of Oklahoma, Norman, (2010)
Gens, A., Sanchez, M., Sheng, D.: On constitutive modeling of unsaturated soils. Acta Geotech. **1**(3), 137–147 (2006)
Hatami, Y.K., Miller, G.A.: Numerical modeling of wetting-inducedsettlement of embankments. GeoCongress 2013, Stability and Performance of Slopesand Embankments III, ASCE, Reston, VA, 333–342 (2013)
Hatami, A., Tourchi, S.: A thermomechanical constitutive model for unsaturated clays. Intl J Geotechn Eng. **12**(2), (2018)
Hatami, K., Granados, J.E., Esmaili, D., Miller, G.A.: Influence of gravimetric water content on geotextile reinforcement pullout resistance in MSE walls with marginal soils. Transp. Res. Rec. **13**(3836), 66–74 (2013)
Ho, H., Hesieh, C.C.: Numerical modeling for undrained shear strength of clays subjected to different plasticity indexes. J Geong. **8**(3), (2018)
Hosseinpour, I., Riccio, M., Almeida, S.S.M.: Verification of the plane strain model for the analysis of encased granular columns. J Geongineering. **12**(4), 137–145 (2017)
Hoyos, L., Pérez-Ruiz, D., Puppala, A.: Refined true triaxial apparatus for testing unsaturated soils under suction-controlled stresspaths. Int. J.Geomech. 281–291 (2012). https://doi.org/10.1061/(ASCE)GM.1943-5622.0000138
Jayanth, S., Kannan, K.R.I., Singh, D.N.: Continuous determination of drying path SWRC of fine grained soils. Geomech Geoeng. Int J. (2012). https://doi.org/10.1080/17486025.2012.727034
Josa, A.: "Un modelo eslastoplastico para suelos no saturados." PhD. thesis, Univ. of Politencnica de Catalunya, Barcelona, Spain, (1988)
Li, L., Aubetin, M.: An analytical solution for the nonlinear distribution of effective and total stresses in vertical backfilled stopes. Geomech Geoeng, Int J. **5**(4), 237–245 (2010)
Lyu S., Hon C.K.H., Chan A.P.C., Wong F.K.W., Javed, A.A.: Relationships among safety climate, safety behavior, and safety outcomes for ethnic minority construction workers. Int'l J. Environmental Reasearch and Public Health. **15**(484) (2018)
Mojezi, M., Biglari, M., Kazem, M., Ashayeri, J.: Determination of shear modulus and damping ratio of normally consolidated unsaturated kaolin. Intl J Geotech Eng. (2018). https://doi.org/10.1080/19386362.2018.1425179
Mun, W., McCartney, J.S.: Compression mechanisms of unsaturated clay under high stress levels. Can. Geotech. J. **52**(12), 2099–2112 (2015)
Nishimura T., Hirabayashi,Y., Delwyn G. Fredlund, Julian K.-M. Gan.: Influence of stress history on the strength parameters of an unsaturated statically compacted soil. Can. Geotech. J. **36**, 251–261 (1999)
Nuth, M., Laloui, L.: Effective stress concept in unsaturated soils: clarification and validation of a unified framework. Int. J. Numer. Anal. Methods Geomech. **32**(7), 771–801 (2008)
Pakbaz, S.M., Alipour, R.: Influence of cement addition on the geotechnical properties of an Iranian clay. Appl Clay Sci. **1**(4), 67–68 (2012)
Power, S.B., Delage, F.P.D.: El Niño–Southern oscillation and associated climatic conditions around the world during the latter half ofthe Twenty-First Century. J. Clim. **31**(15), 6189–6207 (2017)
Rao, R.R., Rahardjo, H., Fredlund, D.G.: Closed form heave solutions for expansive soils. J. Geotech. Eng. **114**(5) (1988)
Roscoe, K.H., Burland, J.B.: On the generalized stress-strain behavior of Wet Clay. Engineering Plasticity, eds: J. Heyman and F. A. Leckie, Cambridge University Press, 535–609 (1968)
Saffih-Hdadi, K., Défossez, P., Richard, G., Cui, Y-J., Tang, A-M., Chaplain, V.: A method to predict the soil susceptibility to compaction of surface layers as a function of water content and bulk density. Soil Tillage Research J. **105**, 96–103 (2009)
Sexton, B.G., McCabe, B.A.: Modeling stone column installation in an elasto visco plastic soil. Intl J Geotech Eng. **9**(5) (2015)
Shen, D., Oki, T., Shingiro, K., Hanasaki, N., Otsomi, N., Kiguchi, M.: Projection of future world water resources under SRES scenarios: an integrated assessment. Hydrological Science J. **59**(10), 1775–1793 (2014)
Sheng, D., Sloan, S.W., Gens, A.: A constitutive model for unsaturated soils: thermomechanical and computational aspects. Comput. Mech. **33**(6), 453–465 (2004)
Sheng D., Zhou A.N.: Coupling hydraulic with mechanical models for unsaturated soils. Can Geotech J. **48**(5), 453–465 (2011)

Vanapalli, S., Oh, W.: A model for predicting the modulus of elasticity of unsaturated soils using the soil-water characteristic curve. Int J Geotech Eng. **4**(4), (2014)
Wheeler S.J., Sharma, R.S., Buisson, M.S.R.: Coupling of hydraulic hysteresis and stress strain behavior in unsaturated soils. Géotechnique. **53**(1), 41–54 (2003)
Wu, Y. X., Shen, S.L., Wu, H.N., Xu, Y.S., Yin, Z.Y., Sun, W.J.: Environmental protection using dewatering technology in a deep confined aquifer beneath ashallow aquifer. Eng. Geol. **196**, 59–70 (2015)
Wu, H.N., Shen, S.L., Yang, J.: Identification of tunnel settlement caused by land subsidence in soft deposit of Shanghai. J. Perform. Constr. Facil. **31**(6) (2017)
Xiong, Y-l., Ye, G-l., Yi, X., Ye, B., Zhang, S., Zhang, F.: A unified constitutive model for unsaturated soil under monotonic and cycling loading. Acta Geotechnica. **14**(3) (2019)
Xu, Y.S., Shen, S.L., Lai, Y., Zhou, A.N.: Design of sponge city: Lessons learnt from an ancient drainage system in Ganzhou, China. J.Hydrol. **563,** 900–908 (2018)
Yegian, M.K., Eseller-Bayat, F.E., Alshawabkeh, A., Ali, S.: Induced-partial saturation for liquefaction mitigation: experimental investigation. J. Geotech. Geoenviron. Eng. **133**(4) (2007)
Zhang, X., Lytton, R.L.: A modified state surface approach on unsaturated soil behavior study. I: basic concept. Can. Geotech. J. **46**(5), 536–552 (2009a)
Zhang, X., Lytton, R.L.: A modified state surface approach on unsaturated soil behavior study. II: general formulation. Can. Geotech. J. **46**(5), 553–570 (2009b)
Zhang, X., Xiao, M.: Using modified state surface approach to select parameter values in the Barcelona basic model. Int. J. Numer. Anal. Methods Geomech. **37**(12), 1847–1866.11 (2013)
Zheng, X., Lytton, R.L.: A modified state surface approach onunsaturated soil behavior study. III: Modeling of coupled hydraumechanicaleffect. Can. Geotech. J. **49**(1) 98–120 (2012)
Zheng, Y., Hatami, K., Miller, G.A.: Numerical modeling of wetting-induced settlement of embankments. GeoCongress 2013, Stability and Performance of Slopes and Embankments III, ASCE, Reston, VA, 333–342 (2013)